10(2013) 1061 – 1079

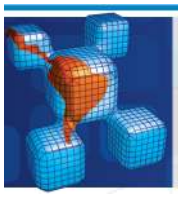

Latin American Journal of Solids and Structures
www.lajss.org

An inverse model for locating skin tumours in 3D using the genetic algorithm with the Dual Reciprocity Boundary Element Method

Abstract

Here, the Dual Reciprocity Boundary Element Method is used to solve the 3D Pennes Bioheat Equation, which together with a Genetic Algorithm, produces an inverse model capable of obtaining the location and the size of a tumour, having as data input the temperature distribution measured on the skin surface.

Given that the objective function, which is solved inversely, involves the DRBEM (Dual Reciprocity Boundary Element Method) the Genetic Algorithm in its usual form becomes slower, in such a way that it was necessary to develop functions based the solution history in order that the process becomes quicker and more accurate.

Results for 8 examples are presented including cases with convection and radiation boundary conditions. Cases involving noise in the readings of the equipment are also considered.

This technique is intended to assist health workers in the diagnosis of tumours.

Keywords

Inverse method, Genetic Algorithm, Dual Reciprocity Boundary Element Method, Tumour, Pennes Bioheat Equation.

Fabrício Ribeiro Bueno[*], [a] **and Paul William Partridge**[b]

[a] Programa de pos-graduação em Estruturas e Construção Civil, Universidade de Brasília, 70910-900 Brasília-DF, Brazil.

[b] Professor, Departamento de Eng. Civil e Ambiental, Universidade de Brasília, 70910-900 Brasília-DF, Brazil.

Received 05 Feb 2012
In revised form 15 Mar 2013

[*]Author email: eng.frb@gmail.com

1 INTRODUCTION

There exist various techniques for the localization of tumours: Invasive techniques, which need surgery and non-invasive techniques, such as ultra sound, MRI and thermal methods. Amongst the non-invasive techniques, thermal methods stand out as economic and safe (Deng and Liu, 2004).

A steady-state mathematical model based on the Bioheat Equation developed by Pennes (1948), simulating heat transfer throughout the human body, was developed by Wissler (1961). These results were compared with experimental data and were considered satisfactory.

Liu and Xu (2000) investigated thermal behaviour in live tissue subject to heating in different ways. One of the means of heating studied is the local heating of the skin due to the presence of skin tumours. For this analysis Liu and Xu used a model based on the Dual Reciprocity Boundary

Element Method, to obtain the temperature distribution at the skin surface. The Boundary Element Method (BEM) is a numerical technique that requires only discretization of the boundary thus reducing the quantity of data necessary to run a problem when comparing to another methods. DRBEM is essentially a generalized way of constructing particular solutions that can be used to solve non-linear and time-dependent problems as well as to represent any integral source distribution (Partridge *et al,* 1992).

Considering these observations Partridge and Wrobel (2007) developed an inverse procedure using the Genetic Algorithm, through which the size and location of a skin tumour could be obtained from temperatures measured at the skin surface in a two dimensional model. These results were later improved by Wrobel *et al* (2009) who implemented in the algorithm the capability of locating tumours with a circular geometry.

The Genetic Algorithm is an optimization method which in the references cited has shown itself to be viable for diagnoses based on thermal information. One of its advantages is that it is unnecessary to supply data on an initial position of the tumour. In addition it is not necessary to calculate sensitivities or search directions.

Here an inverse technique is used, which instead of starting from a tumour for which the size and position are known and the temperature distribution which this provokes on the skin surface calculated, starts from a distribution of temperatures measured in practice by equipment having thermometers created for this purpose, and from this the size and position of the tumour is obtained. The tumour models considered here are in 3D, and not in plane form as in the previous studies, Chan (1992), Deng and Liu (2000), Liu and Xu (2000) and Deng and Liu (2004), Partridge and Wrobel, (2007) and Wrobel *et al* (2009). In this way the results obtained are more complete and satisfactory.

2 PENNES BIOHEAT EQUATION

According to Pennes (1948) the rate of transfer of heat between blood and tissue is proportional to the product of the rate flow of blood and the difference between the temperature of arterial blood and the temperature of local tissue. Thus the bioheat equation was written as follows:

$$h_b = \omega_b \rho_b c_b (1-\kappa)(T_a - T) \tag{1}$$

Where h_b is the rate of transfer of heat per unit volume of tissue, ω_b is the rate of flow of blood per unit volume of tissue, ρ_b is blood density, c_b is the specific heat of blood, κ is a coefficient which takes into account the incomplete thermal equilibrium between tissue and blood, T_a is the arterial blood temperature and T is the local tissue temperature. Pennes considered that κ varies between 0 and 1, however took $\kappa = 0$ for his theoretical curves as has been done by researchers since (Wissler, 1998).

The thermal energy balance for perfusion in the tissue is expressed in the following form:

$$\rho c \frac{\partial T}{\partial t} = k\nabla^2 T + \omega_b \rho_b c_b (T_a - T) + Q \tag{2}$$

Which can be rewritten as:

$$\frac{\rho c}{k}\frac{\partial T}{\partial t} = \nabla^2 T + \frac{\omega_b \rho_b c_b}{k}\left(T_a - T\right) + \frac{Q}{k} \tag{3}$$

Where ρ, c and k represent respectively density, specific heat and thermal conductivity of the tissue and Q is the rate of production of metabolic heat per unit volume of tissue.

Eqn. (3) is subject to the usual boundary conditions for thermal problems:

1º) temperature prescribed $T = \overline{T}$;

2º) heat flux prescribed $q = \overline{q}$;

3º) convection $q = -h_0\left(T - T_0\right)$, where h_0 is the coefficient of heat transfer and T_0 is the temperature of the surrounding fluid;

4º) radiation $q = -\sigma\varepsilon\left(T_r^4 - T^4\right)$, where σ is the Stefan-Boltzman constant and ε is the radiative interchange factor between the surface and the exterior ambient temperature T_r.

For an analysis at a given instant, eqn. (3) should be written in its steady state form, thus becoming:

$$\nabla^2 T = -\frac{\omega_b \rho_b c_b}{k}\left(T_a - T\right) - \frac{Q}{k} \tag{4}$$

Including the constants in (4) one has:

$$\nabla^2 T = -c_1\left(T_a - T\right) - c_2 \tag{5}$$

Where c_1 and c_2 are written as:

$$c_1 = \frac{\omega_b \rho_b c_b}{k}$$

$$c_2 = \frac{Q}{k}$$

Carrying out the multiplication eqn.(5) can also be written as:

$$\nabla^2 T = -c_1 T_a + c_1 T - c_2 \tag{6}$$

Given that T_a is constant, eqn. (6) reduces to:

$$\nabla^2 T = c_3 + c_1 T \tag{7}$$

Where:

$$c_3 = -c_1 T_a - c_2$$

Eqn.(7), considering only constant c_3, is a Poisson equation, and when $c_1 T$ is considered (7) is a Helmholtz equation. The first term is a function of space, and does not include the problem variable, and the second is dependent on the variable T. Here these equations are solved using DRBEM

The values of the parameters necessary to calculate c_1 and c_3 in eqn. (7) were taken from Liu and Xu (2000) as being: $\rho_b = 1000 kg/m^3$, $c_b = 4000 J/(kg^o C)$ and $k = 0.5 W/(m^o C)$, in addition, $\omega_b = 0.0005 ml_b/(ml_t s)$ and $Q = 420 J/(m^3 s)$ for healthy tissue, whilst for tissue with a tumour $\omega_b = 0.002 ml_b/(ml_t s)$ and $Q = 4200 J/(m^3 s)$, in which the subscripts b and t represent blood and tissue, respectively. The temperature of arterial blood is $T_a = 37^o C$.

2.1 Application of DRM to the Bioheat Equation

These equations, Poisson and Helmholtz, are solved separately in Brebbia and Dominguez (1989), where the fundamental solution for isotropic media in 3D $u^* = 1/(4\pi r)$, is employed to deal with the left hand side of eqn. (7) and the right hand side is taken to the boundary using the Dual Reciprocity Method as in Partridge, *et al* (1992), leading to the following system of equations

$$Hu - Gq = (H\hat{u} - G\hat{q})F^{-1}c_3 \tag{8}$$

For the Poisson equation, and

$$Hu - Gq = (H\hat{u} - G\hat{q})F^{-1}uc_1 \tag{9}$$

For the Helmholtz equation.

In this way the matrix equation for the solution of the bioheat equation is

$$Hu - Gq = (H\hat{u} - G\hat{q})F^{-1}c_3 - (H\hat{u} - G\hat{q})F^{-1}uc_1 \tag{10}$$

Where the matrix F is calculated from the approximation function used in the method. Putting $S = (H\hat{u} - G\hat{q})F^{-1}$ one obtains

$$Hu - Gq = Sc_3 - Sc_1 u \tag{11}$$

Reorganizing the matrices

$$(H + Sc_1)u = Gq + Sc_3 \tag{12}$$

Applying the boundary conditions produces the usual system of equations:

$$Ax = y \tag{13}$$

2.2 Application of the convection and radiation boundary conditions

One can consider the boundary condition $q = \overline{q}$ when the skin surface is bandaged. Otherwise it is more realistic to consider convection and radiation boundary conditions, Liu e Xu (2000). The convection and radiation boundary conditions are given by, respectively:

$$q = -h(T - T_0) \tag{14}$$

and

$$q = -\sigma\varepsilon(T^4 - T_r^4) \tag{15}$$

Where $q = K\partial T / \partial n$, $\overline{T}$ and $\overline{q}$ are known values, h is the coefficient of heat transfer, T_0 is the average temperature of the surrounding fluid, σ is the Stefan-Boltzmann constant, ε is the radiative interchange factor between the surface and the exterior environment at temperature T_r

A case considering convection and radiation together can be written:

$$-q = \sigma\varepsilon(T^4 - T_r^4) + h(T - T_0) \tag{16}$$

One can expand the previous equation as follows:

$$-q = \sigma\varepsilon(T^2 + T_r^2)(T + T_r)(T - T_r) + h(T - T_0) \tag{17}$$

The coefficient of apparent heat transfer by radiation for small variations in ambient temperature is $h_r = \sigma\varepsilon(T^2 + T_r^2)(T + T_r)$. Under normal conditions $h_r = 6{,}19\,\mathrm{W/m^2}$ (Liu and Xu, 2000). In this way:

$$-q = h_r(T - T_r) + h(T - T_0) \tag{18}$$

Under the same conditions given above of small variations of ambient temperature for radiation and convection it is possible to consider $T_r = T_0$ which is equivalent to the ambient temperature in question, here taken as T_a = 25ºC. In this way eqn. (18) can be written as:

$$-q = (h_r + h)(T - T_a) \tag{19}$$

According to Liu and Xu (2000), for a preliminary analysis, $h_{ef} = h_r + h = 10\,\mathrm{W/m^2}$. In this way the boundary condition for the elements which are in contact with the external environment is simplified to:

$$q = -h_{ef}\left(T - T_a\right) \tag{20}$$

This value of external temperature is lower than the temperature on the skin surface, which indicates that there will be a reduction in the values of observed temperature.

2.3 Approximation functions and augmentation functions

Bueno and Partridge (2011) considered 3D problems which simulate skin surface temperature using DRBEM with constant triangular boundary elements and tested the use of the following approximation functions $f = r$, $f = r^3$, $f = 1 + r$, $f = 1 + r^3$, $f = r^2 \log r$, and $f = r^4 \log r$, for various cases together with the linear augmentation functions 1, x, y and z, and concluded that the Dual Reciprocity Method produces the best results if the approximation function $f = 1 + r$ is used together with the linear augmentation functions 1, x, y and z.

3 MODELLING THE DIRECT PROBLEM

3.1 Rectangular Model in 3D

The 3D model was constructed in such a way as to permit comparison with the 2D results obtained in previous work, the model has thus the parallelepiped form ABCDEFGH (Fig. 1) representing a sample of skin with a rectangular surface of 0.08 x 0.08 $\mathrm{m^2}$ and a depth of 0.03m.

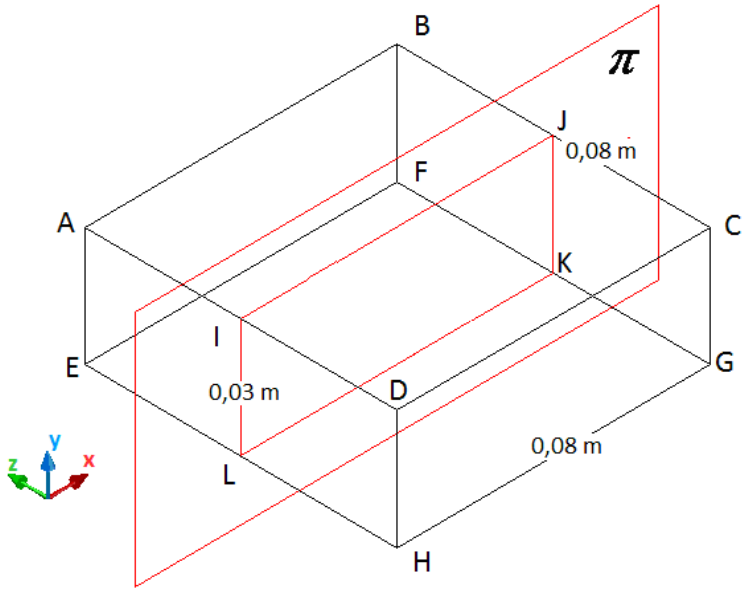

Figure 1 Obtaining the simplified 2D model from the 3D model considered here.

Where the π plane cuts the 3D model one obtains the 2D model studied in previous work

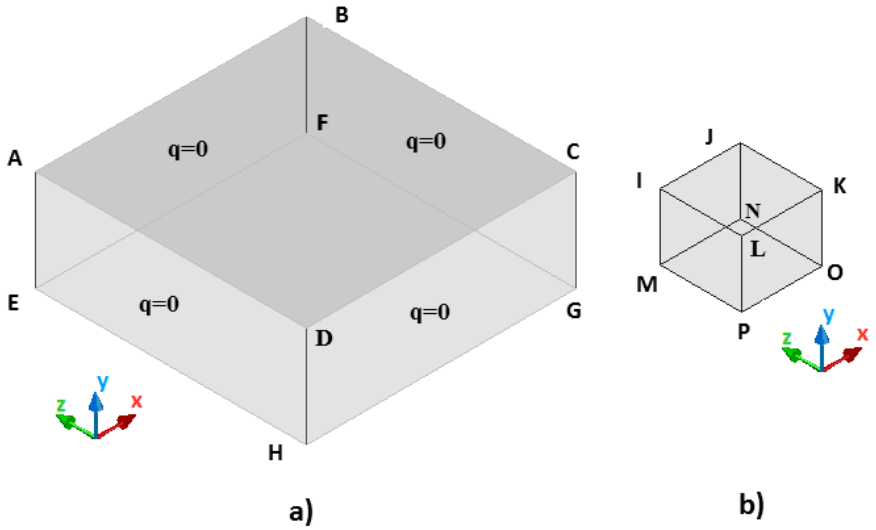

Figure 2 a) Model of healthy tissue in 3D b) 3D rectangular model of tumour.

Fig. 2 (a) shows the 3D representation of the skin tissue delimited by the boundary of the parallelepiped formed by the points A, B, C, D, E, F, G and H defined now as boundary Γ_2. In fig. 2 (b), delimited by the points I, J, K, L, M, N, O and P, one has the 3D model of a tumour of rectangular geometry now called boundary Γ_1. This latter will be in some position inside Γ_2.

Considering boundary Γ_2, the face EFGH is an internal surface and is considered to be at a constant temperature $T = 37^{o}C$ (internal body temperature). The limit ABCD is an external skin surface and can have a boundary condition $q = 0$ if it is considered that the skin is bandaged. Another more realistic boundary condition for ABCD is to consider convection with the external environment. All the other limits of Γ_2 are artificial internal boundaries where the skin sample in question is in contact with other areas of skin and for these cases the boundary condition $q = 0$ is considered. The boundary Γ_1 is considered to be a tumour internal to the boundary Γ_2 where the boundary conditions are that the temperature at a node on Γ_1 is equal to the temperature at the corresponding node on Γ_2 ($T_1 = T_2$) and the exchange of heat done between the two regions is $q_1 = -q_2$.

The discretization into boundary elements was done using 288 constant triangular elements on the Γ_2 boundary and 48 constant triangular elements on the Γ_1 boundary. This kind of elements used was chosen for two basic reasons: 1) It was desired to compare results with the 2D case from Partridge and Wrobel (2007); 2) It was desired to reduce processing time, which due to the combination of the Genetic Algorithm and Dual Reciprocity starred quite high and was reduced to about 20 minutes for one program run.

Initially a rectangular tumour with dimensions 0.02 x 0.02 x 0.01 m^3 and with its centre located at coordinates (0.00; 0.00; 0.01) corresponding to the coordinates x, z and y respectively, as shown in fig. 3.

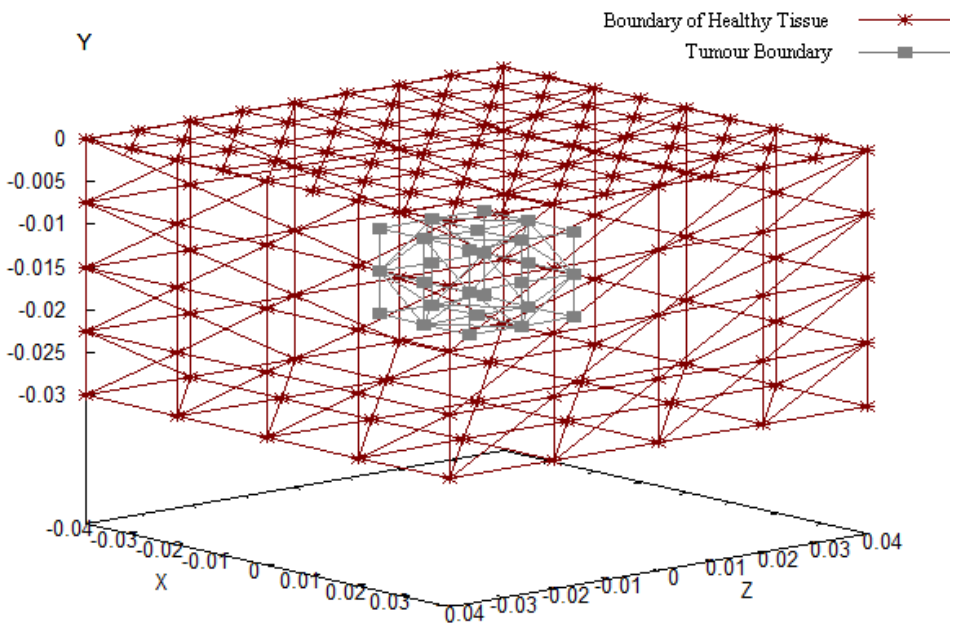

Figure 3 Geometry discretized using constant triangular boundary elements.

In order to find the temperature distribution on the surface ABCD of the tissue (Figs. 1 and 2) the Pennes Bioheat equation is solved using the Dual Reciprocity Boundary Element Method as described above.

3.2 Spherical Tumour Models

Using a similar reasoning, the spherical tumour model can use the same discretization of the healthy tissue (288 constant triangular elements), and the tumour is discretized using 48 constant triangular elements, (Fig. 5).

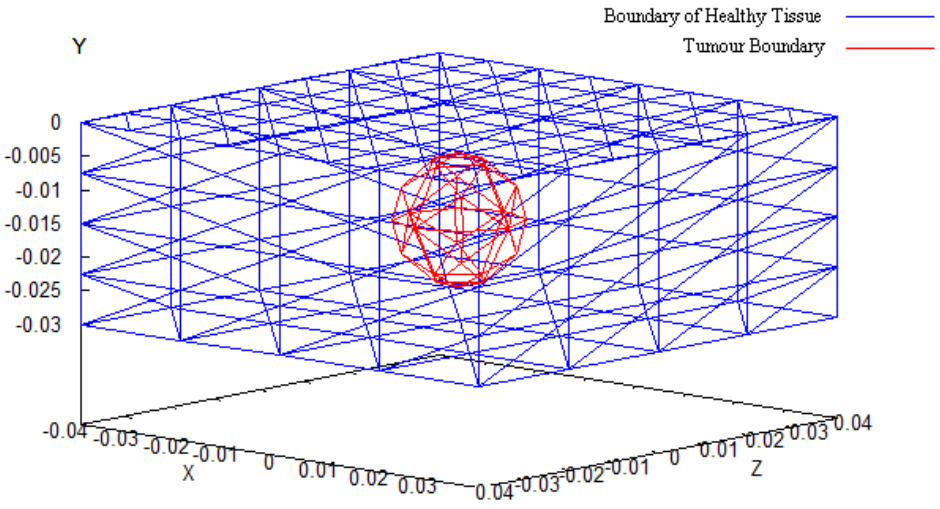

Figure 4 Spherical model of tumour discretized using 48 triangular elements

The values found for the spherical model and those found for the circular model studied by Wrobel *et al* (2009) are compared in table 1.

Table 1 Comparison of the results of the 3D model with those of the 2D model.

Position X	Reference 2D	Sphere	
		Value	Difference
-0.035	37.17256	37.02215	0.4%
-0.030	37.17874	37.03496	0.4%
-0.025	37.19029	37.04777	0.4%
-0.020	37.20861	37.07328	0.4%
-0.015	37.23475	37.09880	0.4%
-0.010	37.26730	37.14506	0.3%
-0.005	37.29831	37.19132	0.3%
0.000	37.31196	37.19152	0.3%
0.005	37.29831	37.19171	0.3%
0.010	37.26730	37.14593	0.3%
0.015	37.23475	37.10014	0.4%
0.020	37.20861	37.07535	0.4%
0.025	37.19029	37.05056	0.4%
0.030	37.17874	37.03900	0.4%
0.035	37.17256	37.02743	0.4%

The distribution of temperature on the surface for the spherical model with its centre at the coordinates (0.00; 0.015; 0.00) and diameter 0.02 m is given in fig. 5.:

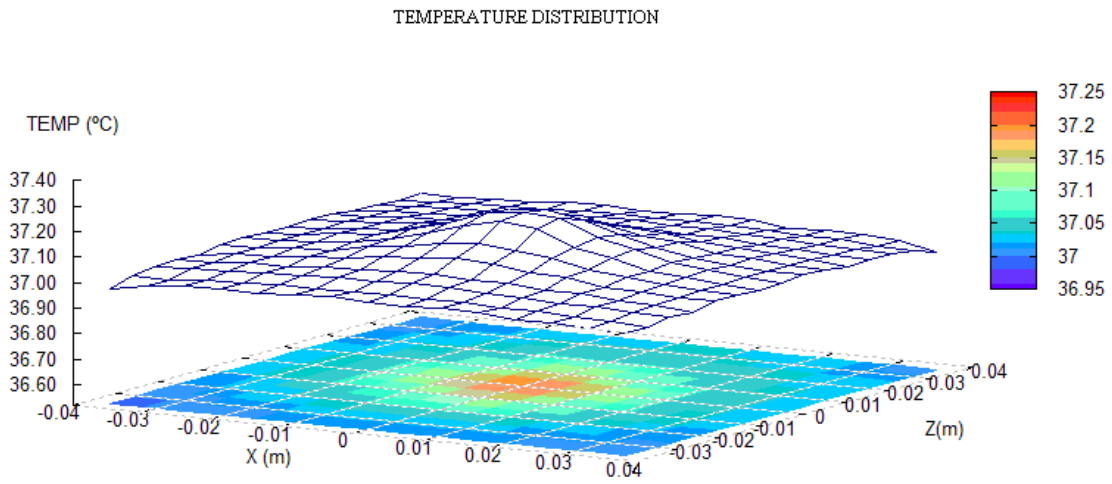

Figure 5 Temperature distribution for the spherical model .

3.3 Convection and radiation boundary conditions

In the following example a 3D model with a rectangular tumour of size (0.02 x 0.01 x 0.02 m^3) centred on (0.00; 0.01; 0.00), is considered, including convective boundary conditions as described above. The results are compared in Table 2 with those of a 2D convective model taken from Partridge and Wrobel (2007).

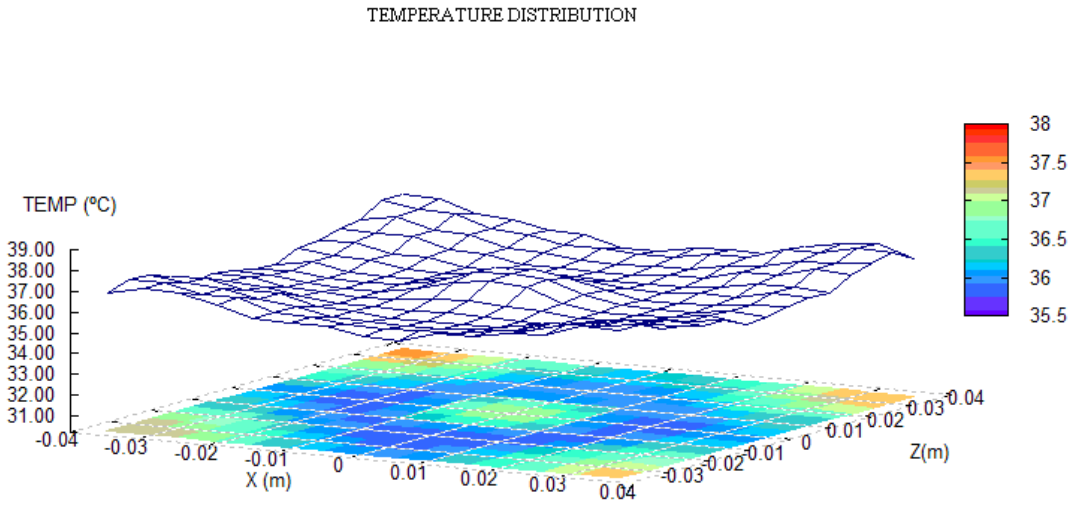

Figure 6 Distribution of temperature for a rectangular convective model.

Table 2 Comparison of the results given by a 3D rectangular convective model with those of a 2D rectangular convective model.

Position X	Reference 2D	3D Model	
		Value	Difference
-0.035	36.4937	36.0609	1.2%
-0.030	36.4108	35.9834	1.2%
-0.025	36.4216	35.9059	1.4%
-0.020	36.4870	35.9406	1.5%
-0.015	36.5951	35.9753	1.7%
-0.010	36.7295	36.4219	0.8%
-0.005	36.8390	36.8685	-0.1%
0.000	36.8777	36.8675	0.0%
0.005	36.8390	36.8666	-0.1%
0.010	36.7295	36.4168	0.9%
0.015	36.5951	35.9671	1.7%
0.020	36.4870	35.9258	1.5%
0.025	36.4216	35.8844	1.5%
0.030	36.4108	35.9497	1.3%
0.035	36.4937	36.0150	1.3%

It can be seen that there is a small difference in the results which may be due to the fact that the discretization in 3D is slightly less refined than in 2D.

Next the formulation of the Genetic Algorithm which determines the location and the size of the tumour is presented.

4 OPTIMIZATION ALGORITHM

Genetic Algorithms are a family of computational models inspired by the natural selection of living beings. These models are created to follow the laws of natural selection guaranteeing the evolution of a given population of individuals (Castro and Partridge, 2006).

Considering five characteristics cited by Lemonge and Barbosa (2004), the Genetic Algorithm employed can be described as follows:

4.1 Genetic representation adopted

Binary Coding, with Chromosomes of 14 digits. These digits have the following meaning:

- 4 digits to represent the x coordinate, one has then $np = 2^4$, or 16 possible solutions for the x coordinate mapped on the interval [- 0.03 ; 0.03] in meters, guaranteeing an accuracy of de +/- 1.875 mm in the results.
- 3 digits for the y coordinate which gives 8 possible solutions, mapped on the interval [0.002 ; 0.026] guaranteeing an accuracy of 1.5 mm in y.
- 4 digits to represent the z coordinate in such a way that there are 16 possible solutions for the z coordinate, mapped on the interval [- 0.03 ; 0.03] in meters thus giving an accuracy of +/- 1.875 mm in the results.
- 3 digits for the size, in such a way that there are 8 possible sizes of rectangular tumour mapped on the interval [0.25 ; 2.00] where the sizes are proportional to the dimensions

0.02 in x, 0.01 in y and 0.02 in z. Thus a tumour described as of dimensions (0.02; 0.01; 0.02) has size 1.00 in the mapping described. A similar scheme was adopted for the spherical models. For the spherical models, a sphere of size 1.00 is a sphere of diameter 0.02m

The chromosome has thus 4 alleles. Thus the 14 digits make possible 16384 different solutions, this then is the size of the search space, and only one of these will be given as an ideal solution. The search space comprises the whole of the region defined above. If the chromosome indicates a tumour which is in a position in which part of the tumour would be outside the search space, this will be automatically eliminated by the fitness function because the temperature distribution will be discontinuous and completely different from a real distribution.

4.2 Initial population

The initial population is created using a subroutine for generating random numbers, (Press *et al*, 1986), in such a way that each digit has a 50% possibility of taking a given binary value (0 or 1). A population with 25 individuals is adopted.

4.3 Fitness function

The objective function should be capable of minimizing the value of the sum of the squares of the differences between the temperatures calculated on surface in ABCD (Fig. 2) and the values of the temperature distribution obtained previously and which correspond to the position and the size of the tumour which it is desired to locate. The chromosomes are put into reverse order according to the value of the objective function and the values of the fitness function are obtained by linear scaling.

4.4 Genetic operators

The individuals which have a greater probability of selection according to the fitness function are selected for crossover, using the roulette wheel method described by Goldberg (1989). Crossover using between four and eight points is carried out between the pairs of chromosomes selected, being one or two per allele.

A process of elitism is employed where the two best individuals in a generation are passed automatically to the next assuring that the best solution is not lost.

4.5 Stopping criteria

Two criteria for stopping were defined:

- Criterion number 1: a maximum of 60 generations is permitted. If the process gets to the last generation, calculations are interrupted and the algorithm returns the best solution obtained up to that moment;
- Criterion number 2: The algorithm will start looping after exploring all of the possible solutions near the best solution obtained, as defined by the function "near search" (to be considered below).

For the Genetic Algorithm used here, in addition to the characteristics common to the majority of such algorithms, new functions were proposed to improve the performance of the same, given difficulties found in obtaining a solution in some cases. In this way the functions "history" and "near search" were created and which are described next.

4.6 History function

In order to avoid repetitive calculations, which arise in the execution of a Genetic Algorithm, a function was created which stores a history of all of the individuals which have been created up to that moment, and before the calculation of the objective function a new individual is submitted to this history. If this individual has a predecessor with the same genetic information, the calculation of the objective function is omitted and the value is attributed which was obtained for the identical predecessor.

The history function also contributes a new possibility of evaluating the efficiency of the algorithm, because it is known that the search space is finite. One form of finding an ideal solution would be to evaluate all of the possible solutions; however this is not viable because of the large number of solutions. In this way, a knowledge of how many individuals were calculated during the optimization process is a good indication of the efficiency of the method.

4.7 Local search function

As has been said above, crossover is one of the principal search processes in a Genetic Algorithm. And this is greatly responsible for exploring unknown regions of the search space. One criticism that can be made of the crossover algorithm is that if two parent individuals contain the same genetic information, two individuals identical to the parents will be generated; this is common in the final stages of the execution of a genetic algorithm. These algorithms generally stop because most of the individuals in the last generation have the same genetic characteristics.

In the first generations this problem is not very perceptible; up to then a small selection pressure is enough to solve the problem, however in the last generations the problem is far more serious. A refined search might not be possible, because the lack of genetic information might indicate a local maximum as the problem solution. Another important fact is that in situations where the function to be optimized has oscillations near the maximum point, the lack of genetic information can again cause the algorithm to select a solution near to the maximum point and not find the true solution exactly.

To solve these two problems the following is proposed: whenever an individual recently created by crossover is identical to an individual that has already existed, (this can be seen by applying the history function), this is substituted by an unused change to the best individual generated up to that moment.

The effect that will be inserted in the Genetic Algorithm is that of a search near the maximum point, preventing convergence up to the point in which all of the points near the best result have been analysed. At this point the algorithm will start to loop because it is no longer possible to find unused individuals near the best solution. In this way the maximum number of attempts to

generate an unused individual should be fixed. One has here a new stopping criterion. Here a maximum of 1000 attempts were considered.

The distance considered in the proximity of the optimum point should be monitored in order that the algorithm does not find just any point in the search space, which might be far from the region being investigated. A maximum distance should be fixed in which the search will be concentrated. The maximum distance used here is 1 position for the variables y and "size" which use alleles of three digits and two positions for the variables x and z which use alleles of 4 binary digits. By position here it is meant one or two binary intervals as defined in section 4.1. This function is only used intensively when the algorithm initiates the process of convergence. In this way the "local search" function does not diminish the search capacity of the Genetic Algorithm but adds at the final stage a capacity for refining the solution, in addition to reducing the large quantities of repeated calculations that the Genetic Algorithm executes in the final stage of convergence.

5 RESULTS

5.1 Inverse problem in the general formulation

Case 1: Rectangular Tumour, 0.02x0.01x0.02m, centred at (0.00; 0.01; 0.00)m.

After 6 generations it was already possible to observe the presence of the ideal solution amongst the 25 individuals in the population, as a consequence this solution was present in all the future generations. The algorithm stopped after 51 generations because stopping criterion 2 had been reached. The history function counter indicated that 951 possible solutions of a total of 16384 had been calculated, which shows the efficiency of the search method.

The solution found was a tumour with dimensions 0.02 x 0.01 x 0.2 m centred on (0.0; 0.11; 0.00), which produced the temperature distribution given in fig. 7 (found), compared with the original distribution (expected).

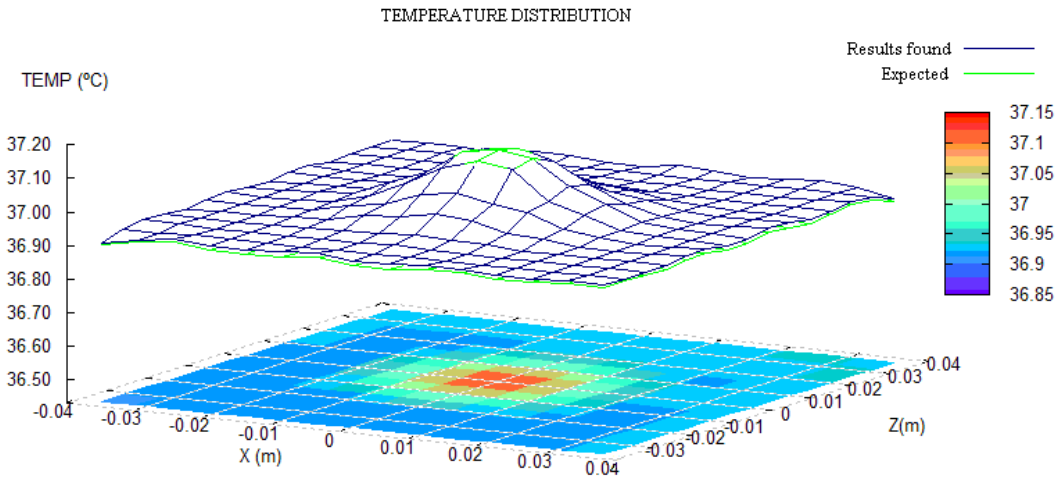

Figure 7 Comparison of the temperature distributions found and expected for case 1.

It can be seen that there is a small difference between the results found and those expected, due to the fact that the binary mapping of the variables is not capable of representing exactly the expected value. The accuracy of the approach is discussed above. However it can be noted that this small difference does not affect the quality of the solution found.

Case 2: Rectangular tumour, 0.03x0.015x0.03m centred at (0.01125; 0.0011; 0.01125)m.

In this case 40 generations were necessary for the algorithm to find the ideal solution. Calculations ceased after 50 generations because stopping criterion 2 was reached with a total of 903 individuals analysed.

The solution found was a tumour with dimensions equal to those expected which could be represented exactly. The dimensions were 0.03 x 0.015 x 0.03 m centred at (0.01125; 0.0011; 0.01125).

Case 3: Spherical tumour, diameter 0.02 m, centred at (0.00; 0.01; 0.00)m.

The ideal solution appeared in the population after 12 generations. The algorithm stopped after 60 generations because stopping criterion 1 was reached (Maximum number of generations). The counter in the History Function indicated that 1119 possible solutions of a total of 16384 were calculated. The solution found was a tumour with a diameter of 0.02 m centred on (0.00; 0.011; 0.00), which produced the temperature distribution shown in fig. 8 in which the distribution found is compared with the expected distribution.

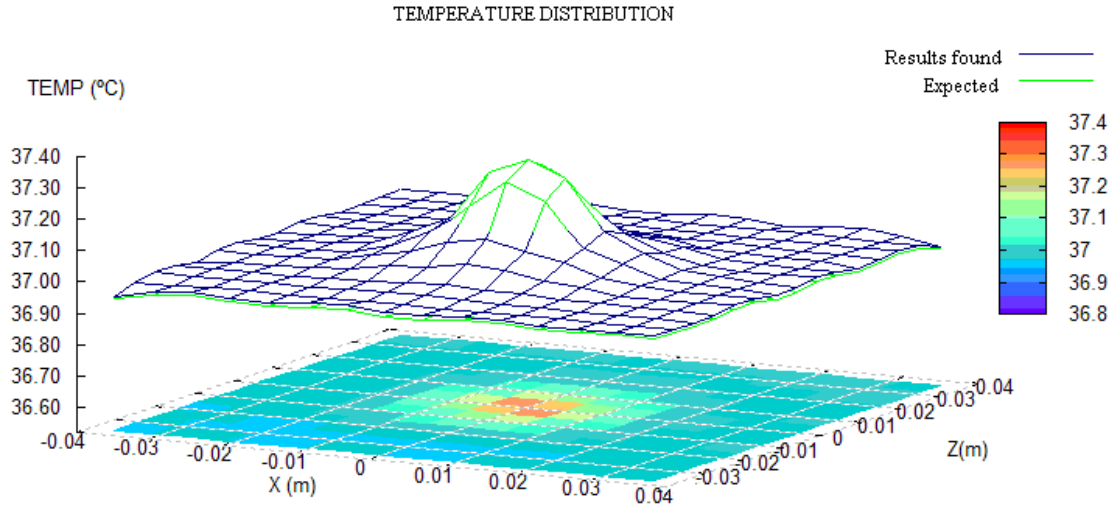

Figure 8 Comparison of found and expected temperature distributions for case 3.

Case 4: Spherical tumour diameter 0.02 m, centred at (-0.015; 0.02; 0.01125)m.

The solution appeared in the population after 19 generations. Calculations ceased after 46 generations when stopping criterion 2 was reached, the History Function showed that 830 individuals

had been analysed. The solution found was a tumour with the dimensions expected which could be represented exactly.

5.2 Cases considering convection and radiation

Convection and radiation can be considered together in order to obtain a more realistic boundary condition when the skin surface is exposed.

Case 5: Rectangular tumour, 0.035x0.0175x0.035m centred at (0.00; 0.02; 0.0125)m.

The ideal solution appeared amongst the population after 24 generations. Calculations ceased after 43 generations because stopping criterion 2 was reached with a total of 783 individuals analysed. The solution found was a tumour with dimensions exactly equal to those expected.

Case 6: Spherical tumour, diameter 0.015 m centred at (0.00375; 0.008; 0.0075)m.

After 24 generations the presence of the ideal solution could be observed amongst the individuals of the population. Calculations ceased after 38 generations because stopping criterion 2 was reached after the whole of the neighbourhood of the optimum point had been explored with the analysis of 698 individuals. The solution found was identical to that expected.

5.3 Consideration of errors in measurements

Equipment for measuring temperature on the skin surface was studied in the medical literature by (Togawa, 1985). It is known that such equipment has an error of the order of 0.05 ºC for older equipment and 0.04 ºC for commercial quartz crystal oscillators, being as little as 0.02 ºC for modern equipment using infrared radiation.

To simulate temperature measurement on the skin surface and evaluate the capacity of the Genetic Algorithm to take in to account the accuracy of existing equipment, errors were introduced into the observed temperature data in a random way (Press *et al*, 1986) The standard deviation was monitored in such a way that the most accurate readings had an error of 0.01 ºC and the least accurate 0.06 ºC.

Case 7: Rectangular tumour 0.02x0.01x0.02 m centred at (0.00; 0.011; 0.00), measurement error $\sigma = 0.0267$ ºC.

After 26 generations the presence of the solution can be observed amongst the 25 individuals of the population. Calculations ceased after 55 generations because stopping criterion 2 was reached. The counter in the history function indicates that 955 individuals of a possible 16384 were calculated. The solution found was a tumour with dimensions equal to those expected. The temperature distributions are shown in fig. 9 in which the results found are compared with the expected values.

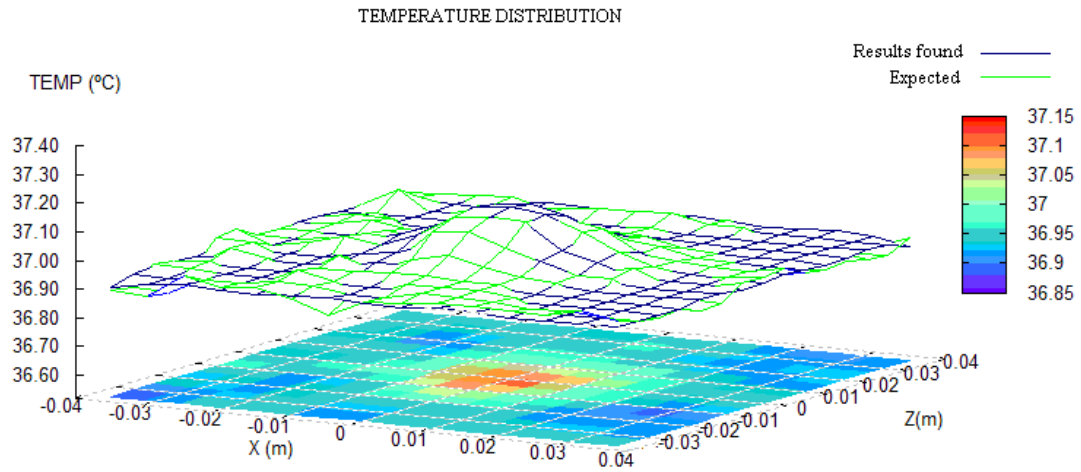

Figure 9 Comparison between the found and expected temperature distributions for case 7.

Case 8: Spherical tumour, diameter 0.015 m, centred at (0.00375; 0.008; 0.0075), standard deviation $\sigma = 0.0178$ ºC, considering convection and radiation

The solution appeared amongst the population after 6 generations. Calculations ceased after 41 generations when stopping criterion 2 was reached. The counter in the history function indicated that 760 possible solutions were calculated of a total of 16384. The tumour found had dimensions equal to those expected.

6 CONCLUSIONS

6.1 Discussion

In cases 1 and 3 the difference in the results for the y coordinate is due to the binary mapping which, in the way in which it was defined, has an accuracy of 0.0015 m.

The Genetic Algorithm may find the solution to the problem in the first few generations, as happens for example, in case 1, where the solution appears amongst the population at generation 6. However to guarantee that this really is the best solution it is necessary to execute more generations. Calculations stopped at generation 51. The number of generations was small confirming the correct dimensioning of the Genetic Algorithm.

The addition of noise to the input data, with the intention of simulating imperfections in the equipment used for measuring the temperatures, did not alter the capacity of the algorithm to find accurate solutions (cases 7 and 8).

The implementation of boundary conditions in convection and radiation associated with the addition of noise to the input data did not generate interference in the results obtained in Case 8, given that this example considers the same tumour as case 6 and in both cases the same solution was obtained even with the same errors due to the mapping of variables.

6.2 Conclusions

The Boundary Element Method shows itself to be viable for the solution of inverse problems with the Genetic Algorithm in 3D. It should be noted that the method does not need to remesh for each new individual considered as would be the case with domain methods.

The Genetic Algorithm in its traditional form carries out many repeated calculations which is a limiting factor in the case of DRBEM. This problem was tackled by the addition of functions which avoid the reprocessing of individuals which have been calculated before and effort was concentrated on searching for possible solutions in the vicinity of the best solution found up to the moment. These routines permitted a large reduction in processing time and also permitted the algorithm to succeed in some cases where it would have failed.

A population of 25 individuals was only possible for a problem with 4 variables due to the efficiency of the functions "history" and "near search" developed here.

Thermal methods are an alternative for aiding health workers in the diagnosis of tumours and also show themselves to be a solution for accompanying the treatment of the same.

The Genetic Algorithm used here was developed for the problem of the localization of tumours; however the same can be used with other types of optimization problems. The functions implemented can bring benefits for the general use of the Genetic Algorithm.

References

[1] WROBEL, L. C.; PARTRIDGE, P. W.; DE CASTRO, L. C. L. B.; BUENO, F. R. A BEM technique for the detection of skin tumours by thermal analysis. In: UK Conference on boundary integral methods, 7, *Proceeding.* Nottingham, p. 99 – 106, 2009.

[2] BUENO, F. R.; PARTRIDGE, P. W. A study of dual reciprocity for three dimensional models applied to the solution of Pennes Bioheat equation. In: Beteq, XII, 2011, *Proceedings...* Brasilia, p. 182-189, 2011.

[3] CHAN, C. L. Boundary element method analysis of the bioheat transfer equation. *Journal of Biomechanical Engineering*, v. 114, p. 358–365, 1992.

[4] DE CASTRO, L. C. L. B.; PARTRIDGE, P. W. Minimum weight design of framed structures using a genetic algorithm considering dynamic analysis. *Latin American Journal of Solids and structures*, v. 3, p. 107–123, 2006.

[5] DENG, Z. S.; LIU, J. Modelling of multidimensional freezing problem during cryosurgery by the dual reciprocity boundary element method. *Engineering Analysis with Boundary Elements*, v. 28, p. 97–108, 2004.

[6] DENG, Z. S.; LIU, J. Parametric studies on the phase shift method to measure the blood perfusion of biological bodies. *Medical Engineering & Physics*, v. 22, p. 693–702, 2000.

[7] GOLDBERG, D. E. *Genetic algorithms in search, optimization and machine learning*. 1st ed. Boston: Addison Wesley Longman Publishing Co., 1989.

[8] LEMONGE, A. C. C.; BARBOSA, H. J. C. An adaptive penalty scheme for genetic algorithms in structural optimization. *International Journal for Numerical Methods In Engineering*, v. 59, p. 703-736, 2004.

[9] LIU, J.; XU, L. X. Boundary information based diagnostics on the thermal states of biological bodies. *International Journal of Heat and Mass Transfer,* v. 43, p. 2827–2839, 2000.

[10] PARTRIDGE, P. W.; WROBEL, L. An inverse geometry problem for the localisation of skin tumours by thermal analysis. *Engineering Analysis with Boundary Elements*, v. 31, p. 803-811, 2007.

[11] PARTRIDGE, P. W.; WROBEL, L. C; BREBBIA, C. A. *The dual reciprocity boundary element method*. London: Elsevier Applied Science; Southampton: Computational Mechanics Publications, 1992.

[12] PENNES, H. H. Analysis of tissue and arterial blood temperatures in the resting human forearm. *Journal of Applied Physiology*, v. 1, n. 2, p. 93–122, 1948.

[13] PRESS, W. H., FLANNERY B. P.; TEUKOLSKY, S. A.; VETTERLING, W. T. *Numerical recipes:* the art of scientific computing. 1st ed. Cambridge: Cambridge University Press, 1986.

[14] TOGAWA, T. Body temperature measurement. *Clinical Physics and Physiological Measurement*. v. 6, n. 2, p. 83-108, 1985.

[15] WISSLER, E. H. Pennes' 1948 paper revisited. *Journal of Applied Physiology*, v. 85, p. 35-41, 1998.

[16] WISSLER, E. H. Steady-state temperature distribution in man. *Journal of Applied Physiology*, v. 16, p. 734–740, 1961.